Pedestal-top n_e control using RMP at KSTAR

Minseok Kim[1], SangKyeun Kim[2], Keith Erickson[2], Andy Rothstein[1], Youngho Lee[3], Hyunsun Han[3], ChangMin Shin[4], JungHoo Hwang[3,4], Azarakhsh Jalalvand[1], Peter Steiner[1], Ricardo Shousha[2], CheolSik Byun[1], Jalal Butt[1], Sang-hee Hahn[3], June-Woo Juhn[3], Boseong Kim[3,5], SeongMoo Yang[2], Qiming Hu[2], David Eldon[6], Nikolas Logan[7], and Egemen Kolemen[1,2]

[1]Department of Mechanical & Aerospace Engineering, Princeton University, Princeton, NJ, 08540, USA [2]Princeton Plasma Physics Laboratory, Princeton, NJ, 08540, USA
[3]Korea Institute of Fusion Energy, Daejeon 34133, Republic of Korea [4]Department of Nuclear and Quantum Engineering, KAIST , Daejeon, 34141, Republic of Korea
[5]Department of Nuclear Engineering, Seoul National University, Seoul, 08826, Republic of Korea [6]General Atomics, San Diego, CA, 92121, USA
[7]Department of Applied Physics, Columbia University, New York, NY, 10027, USA

Control & Operation of Tokamaks 2025, Lausanne, Switzerland, February 03 – 14, 2025

E-mail: mseokim@princeton.edu

Introduction

1. **Electron density profiles can be reconstructed using five channels of the two-colored interferometer (TCI) [1].**
2. **The reconstruction algorithm can be accelerated by using a neural network, enabling real-time density profile control in KSTAR.**
3. **Pedestal-top electron density can be controlled using RMP.**

1. Electron density profile reconstruction model

(a) Edge model: $a_1\left[\gamma+\frac{1-\gamma}{2}\left(1-\frac{\tanh(\frac{\psi-\psi_m}{\Delta/2})}{\tanh(1)}\right)\right]$

(b) Core model: $a_2\left|1-\left(\frac{\psi}{\psi_t}\right)^{a_3}\right|^{a_4}$

- ψ : Normalized poloidal flux function
- ψ_m : Position of the middle of the pedestal $(\psi_m = 1-\Delta/2)$
- Δ : Pedestal width
- a_1 : Plasma density at the pedestal top
- γ : The ratio of electron density between pedestal top and LCFS

- ψ_t : Position of the pedestal top $(\psi_t = 1-\Delta)$
- a_2 : The difference of the plasma density between axis and pedestal top
- a_3 : Fitting coefficient in the core region
- a_4 : Fitting coefficient in the core region

(c) Scrape-off layer multiplier: $4-3\psi$

$$s(\psi)=\begin{cases}1 & (1\geq\psi\geq 0)\\ 4-3\psi & (\psi>1)\end{cases}$$

(d)
$$n_{e0}(\psi)=\begin{cases}\text{Edge model} & (\psi\geq\psi_t)\\ \text{Edge model + Core model} & (\psi<\psi_t)\end{cases}$$

$$n_e(\psi)=n_{e0}\times s$$

< Fig.1. Descriptions of the fitting model >

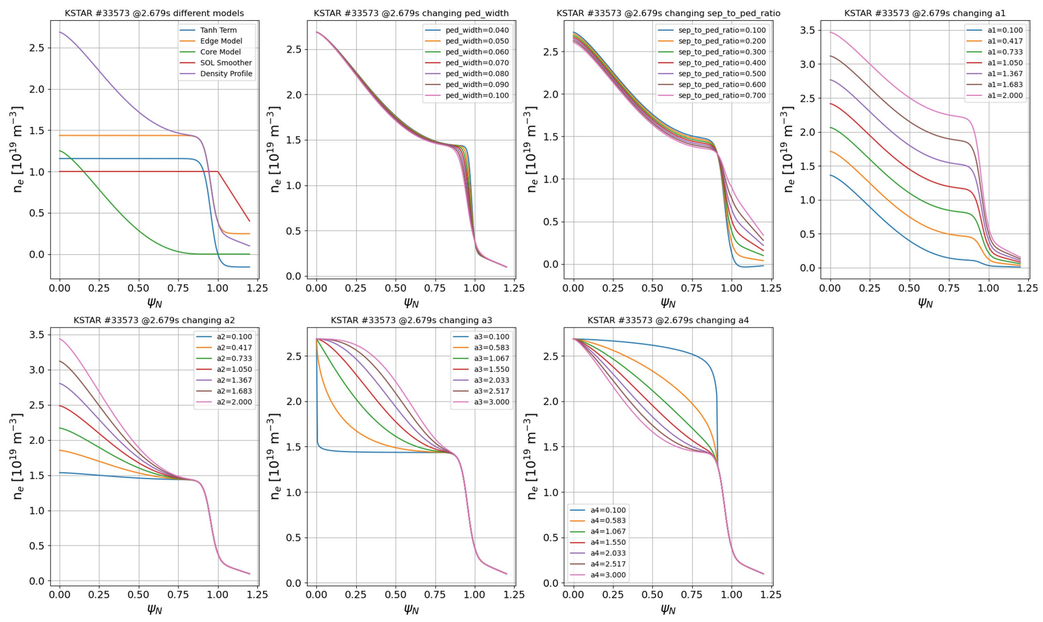

< Fig.2. Sensitivity check of the model >

2. Parametrize flux mapping to real-space

R : spatial domain from 1.1 to 2.4 (33 points)

$R < R_{axis}$: $R2=\frac{(R-R_{axis})}{(R_{axis}-R_{in})}$, $y=b_1\times R2^2+(b_1-1)\times R2^3$

$R \geq R_{axis}$: $R2=\frac{(R-R_{axis})}{(R_{out}-R_{axis})}$, $y=b_2\times R2^2+(1-b_2)\times R2^3$

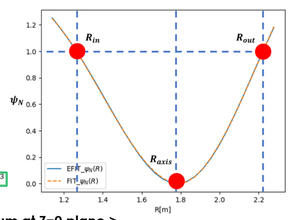

< Fig.3. Equilibrium at Z=0 plane >

3. Fitting the model with TCI

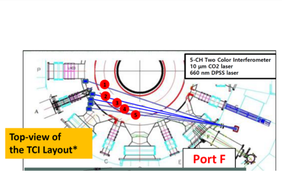

< Fig.4. Top view of TCI at KSTAR >

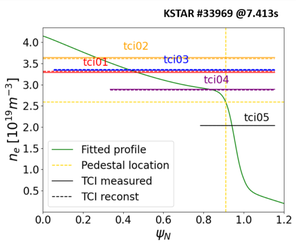

< Fig.5. Reconstructed ne profiles >

4. Neural network with 2022 and 2023 KSTAR data

```
Model: "sequential"
_________________________________________________________________
Layer (type)                 Output Shape              Param #
=================================================================
dense (Dense)                (None, 20)                220
_________________________________________________________________
batch_normalization (BatchNo (None, 20)                80
_________________________________________________________________
activation (Activation)      (None, 20)                0
_________________________________________________________________
dense_1 (Dense)              (None, 20)                420
_________________________________________________________________
batch_normalization_1 (Batch (None, 20)                80
_________________________________________________________________
activation_1 (Activation)    (None, 20)                0
_________________________________________________________________
dense_2 (Dense)              (None, 4)                 84
_________________________________________________________________
batch_normalization_2 (Batch (None, 4)                 16
_________________________________________________________________
activation_2 (Activation)    (None, 4)                 0
=================================================================
Total params: 900
Trainable params: 812
Non-trainable params: 88
_________________________________________________________________
```

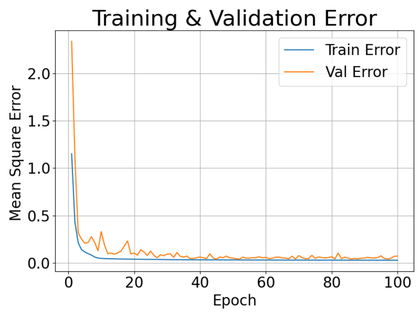

< Fig.6. Training summary >

1. **Training: 2022 KSTAR [93,812 ($\sim 10^5$)]**
2. **Val: Half 2023 KSTAR [33,591 ($\sim 10^5$)]**
3. **Test: Half 2023 KSTAR [33,591 ($\sim 10^5$)]**

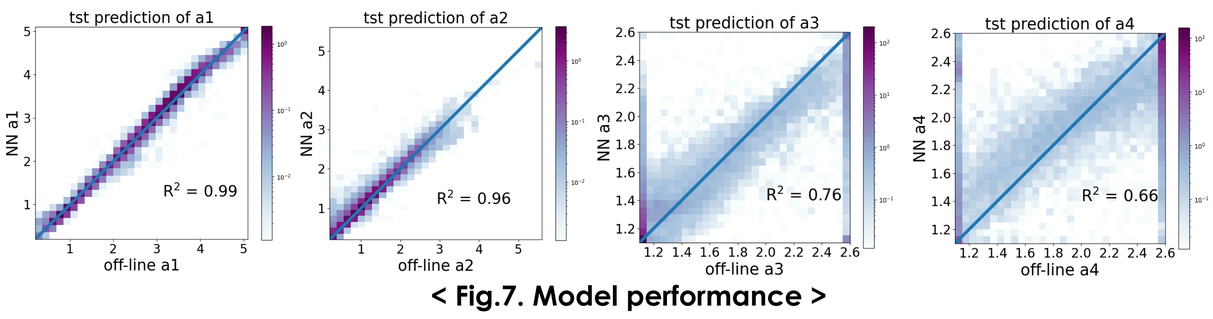

< Fig.7. Model performance >

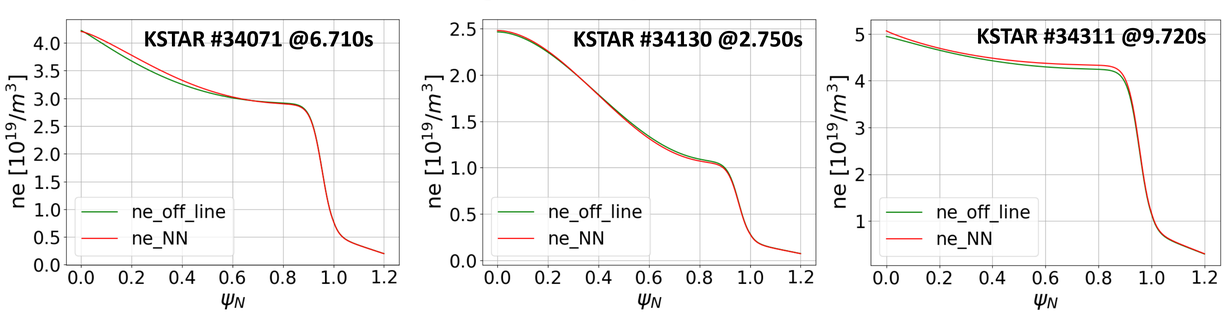

< Fig.8. Prediction results >

5. Controller design

Transfer function

e^{st} ($s=(\sigma+i\omega)$) → $H(s)$ → $H(s)e^{st}$

Impulse response

$$H(s)=\frac{K}{1+sT} \xrightarrow{\text{Inverse L.T.}} h(t)=\frac{K}{T}e^{-\frac{t}{T}}$$

Output in time -domain

$$y(t)=h(t)*u(t)=\int_0^\infty h(\tau)u(t-\tau)d\tau$$

System identification

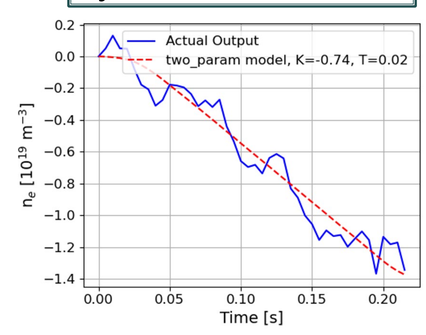

Closed -loop system

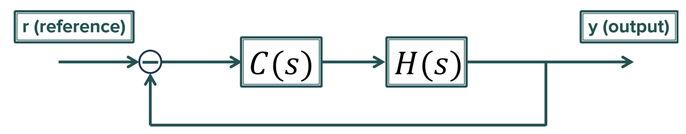

$$C(s)=K_p+K_i\frac{1}{s} \Rightarrow Y(s)=\frac{HC}{1+HC}R(s)$$

G(s): Closed-loop transfer function

$$G(s)=\frac{K/T(K_ps+K_I)}{s^2+\underbrace{[(K\cdot K_p+1)/T]}_{2\zeta\omega_0}s+\underbrace{K\cdot K_I/T}_{\omega_0{}^2}}$$

$$K_p=\frac{1}{K}=-1.35$$

$$K_I=\frac{1}{KT}=-57.4$$

Place pole to be as same as plant pole

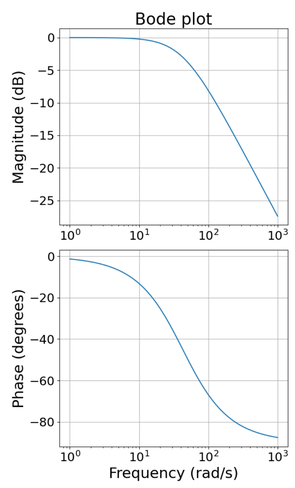

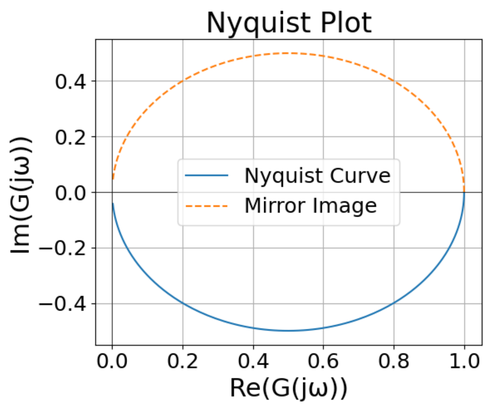

< Fig.9. Bode and Nyquist plots of G(s) >

6. PI controller results

No PVD @KSTAR #36999 | **PVD D2 0.3V @KSTAR #37086** | **PVD D2 0.3V @KSTAR #37096**

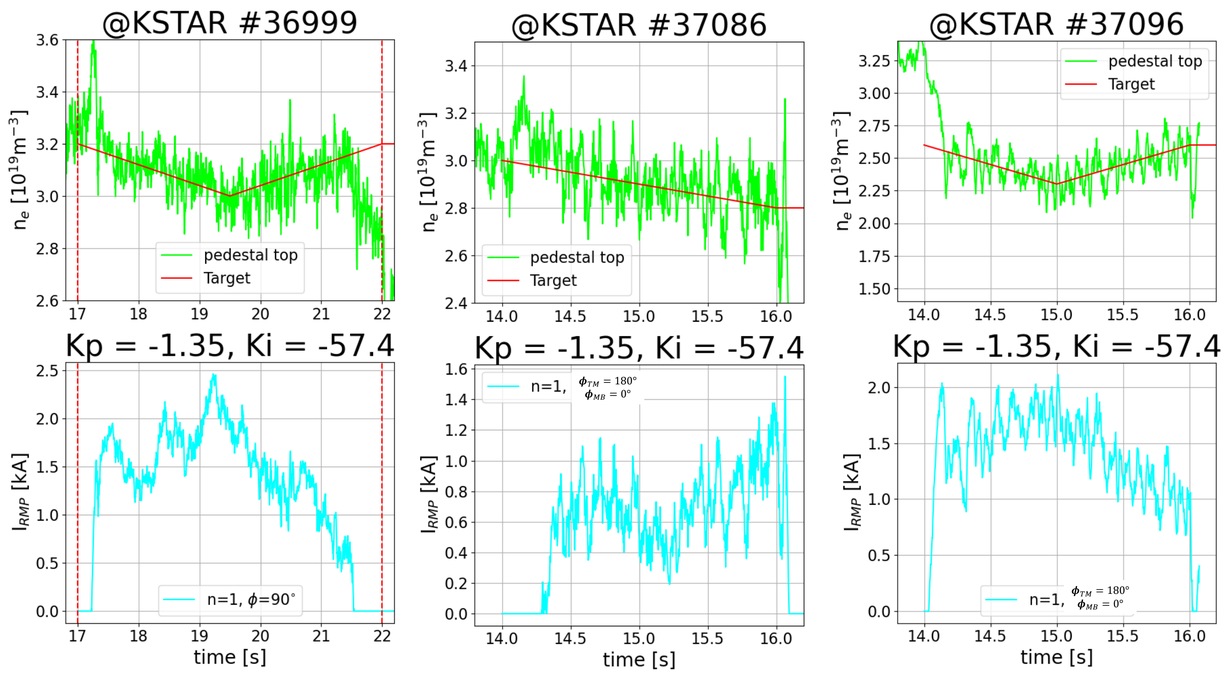

< Fig.10. Pedestal-top ne control >

7. Conclusion & Future work

1. **Real-time electron density profile reconstruction algorithm has been implemented in the KSTAR PCS.**
2. **The density at ψ_N=0.9 could be controlled by using RMP.**
3. **Full profile controller with multiple actuators including RMP, Gas, SMBI, and Pellet will be tested.**

Acknowledgement

1. Lee, S. G., et al. "Overview and recent progress of KSTAR diagnostics." *Journal of Instrumentation* 17.01 (2022): C01065.
2. Snyder, P. B., et al. "ELMs and constraints on the H -mode pedestal: peeling –ballooning stability calculation and comparison with experiment." *Nuclear fusion* 44.2 (2004): 320.
3. C.W.Rowley, "Introduction to Feedback Control", Princeton University Press, 2024

4. Minseok is pleased to acknowledge that the work reported on in this paper was substantially performed using the Princeton Research Computing resources at Princeton University which is consortium of groups led by the Princeton Institute for Computational Science and Engineering (PICSciE) and Office of Information Technology's Research Computing.

This work was funded by the U.S. Department of Energy, Office of Fusion Energy Science, DE-SC0020357